Author Manuscript

Author Manuscript

Author Manuscript

Author Manuscript

HHS Public Access

Author manuscript

Biomed Microdevices. Author manuscript; available in PMC 2017 August 29.

Published in final edited form as:

Biomed Microdevices. 2016 April ; 18(2): 24. doi:10.1007/s10544-016-0046-2.

A Dual Wedge Microneedle for sampling of perilymph solution via round window membrane

Hirobumi Watanabe[*],
Department of Mechanical Engineering, Columbia University, 500 West 120th Street, New York, NY 10027, USA

Luis Cardoso,
Department of Biomedical Engineering, The City College of The University of New York, New York, NY 10031, USA

Anil K. Lalwani, and
Department of Otolaryngology - Head and Neck Surgery, Columbia University College of Physicians and Surgeons, New York, NY 10032, USA

Jeffrey W. Kysar
Department of Mechanical Engineering, Columbia University, 500 West 120th Street, New York, NY 10027, USA

Abstract

Objective—Precision medicine for inner-ear disease is hampered by the absence of a methodology to sample inner-ear fluid atraumatically. The round window membrane (RWM) is an attractive portal for accessing cochlear fluids as it heals spontaneously. In this study, we report on the development of a microneedle for perilymph sampling that minimizes size of RWM perforation, facilitates quick aspiration, and provides precise volume control.

Methods—Considering the mechanical anisotropy of the RWM and hydrodynamics through a microneedle, a 31G stainless steel pipe was machined into wedge-shaped design via electrical discharge machining. Guinea pig RWM was penetrated *in vitro*, and 1 μ1 of perilymph was sampled and analyzed via UV-vis spectroscopy.

Results—The prototype wedge shaped needle created oval perforation with minor and major diameter of 143 and 344 μm (n=6). The sampling duration and standard deviation of aspirated volume were seconds and 6.8% respectively. The protein concentration was 1.74 mg/mL.

Conclusion—The prototype needle facilitated precise perforation of RWMs and rapid aspiration of cochlear fluid with precise volume control. The needle design is promising and requires testing in human cadaveric temporal bone and further optimization to become clinically viable.

Index Terms

Personalized medicine; inner ear disease; minimally invasive sampling; microneedle

[*]Corresponding author: hw2420@columbia.edu.

Author Manuscript Author Manuscript Author Manuscript Author Manuscript

I. Introduction

Inner ear diseases such as hearing loss and balance disturbance are common and negatively impact on quality of life. Despite significant research and innovation, patient specific treatments for inner ear illnesses such as sudden or progressive sensorineural hearing loss (SNHL), hereditary hearing impairment, Ménière's disease, and others remain elusive — steroids are generically and nonspecifically used for a multitude of cochleovestibular diseases with limited proven efficacy. This is due to the inability of the physician to determine the etiology of patient's symptoms due to the anatomic inaccessibility of the cochlea; in absence of specific diagnosis, targeted "precision" medicine is not possible.

This limitation could, in part, be overcome with the ability to sample cochlear fluid for diagnostic purposes. Within the cochlea, the scala tympani and scala vestibuli are connected to each other through the helicotrema at the apex of the cochlea and are filled with perilymph solution; the scala media, or the middle chamber contains endolymph. The scala media is connected to the vestibular system via ductus reuniens. Additionally, near the RWM, the scala tympani has another opening, namely, cochlear aqueduct, which is connected to subarachnoid space filled with cerebrospinal fluid. Perilymph and endolymph are critical in creating the ionic environment for the transduction of air vibrations into neural signals via the hair cells and providing nutrients for these cells from vasculature. When a patient has an acute or chronic illness of inner ear, it is likely to be reflected by abnormalities in the chemical make-up of the solution, with changes in the presence or concentration of various ions, proteins, bacteria, or viruses when compared to healthy perilymph (1-6).

An effective sampling method of the perilymph through the RWM would make possible electrolytic, nucleic and proteomic analysis via a variety of techniques including polymerase chain reaction, immunochemistry, and liquid chromatography–tandem mass-spectrometry (LC-MS/MS), among others. Previously, researcher have shown that 1 μl of perilymph, collected from patients undergoing cochlear implantation or tumor resection with glass capillary, is sufficient to perform proteomic analysis (11). In animals, the glass capillary has also been used to collect perilymph samples to investigate pharmacokinetics and hydrodynamics of the inner ear. In guinea pig, it was shown that perforation in the RWM induces perilymph outflow driven by the CSF pressure and 1 μl of sampled solution contains 20% of CSF. These procedures using glass capillary present 3 engineering opportunities that can be improved, i.e., simplicity, duration and reliability of the procedure. First, the glass capillary cannot be used to make the perforation in the RWN and was used only to aspirate after the creation of the hole. Second, the small pore size at risk of clogging and restricts the speed of aspiration down to 1 μl/min. Lastly, the glass is a brittle material and therefore may crack or break {Hara, 1989 #80}.

In this study, we report on a new design for a micro-needle suitable for aspiration of cochlear fluid through RWM. The design objectives for this micro-needle were for it to facilitate smooth penetration of the RWM with minimal damage, and to subsequently aid in aspiration of precise volume of perilymph in minimal time. The micro-needle was designed based on the mechanical properties of the RWM, microanatomy of the human ear, and the

Author Manuscript Author Manuscript Author Manuscript Author Manuscript

hydrodynamics of aspiration. Stainless steel was selected as the needle material due to its strength and biocompatibility. The prototype needle built with electrical discharge machining was evaluated with white light laser interferometry and assembled with a micropipette to sample perilymph solution from guinea pig cochlea *in vitro*. The perforation in the RWM was assessed via electron microscopy. The aspirated solution was analyzed using ultraviolet visible (UV-vis) spectroscopy to confirm that perilymph solution was successfully sampled.

II. Materials and Methods

A. Design of a dual wedged needle

To design a needle optimized for the creation of a minimally traumatic hole, the mechanical properties of the RWM was considered. Unlike what the name suggests, the RWM actually has an oval shape in a planar view and is woven with nano-meter scale collagen fibers. These fibers run parallel to the major axis of the oval, resulting in the property called anisotropy whereas the RWM is stronger in the major axis orientation than in the minor axis. Consequently, a perforation with a regular round needle, such as a hypodermic needle, results in an asymmetric oval shape. Usually, the size of the hole is larger than the needle because the pre-tension in the RWM tends to expand the perforation.

By taking advantage of the anisotropy and minimizing the effect of pre-tension, we designed a needle that makes a linear incision along the direction of the collagen fibers to reduce the energy of perforation and consequently minimize the trauma and facilitate the subsequent healing process. Figure 1 shows the design of the dual wedge needle. The standard anatomical terms of location were borrowed to define the direction. In the frontal plane view, the needle has a tip with two blades. In the longitudinal plane view, these two blades are aligned in the center of the needle making the shape of one symmetrical wedge. These two linear blades are intended to sever the collagen fibers parallel to them and use the wedge to open the linear incision to allow for making a hole with the minimum size necessary for the aspiration of the perilymph solution. The angle of the wedge was minimized for small force penetration.

To determine the appropriate length of the needle that would allow aspiration of perilymph while avoiding contact with the inner ear wall and basilar membrane, a micro CT scan of human temporal bone was performed. A fresh temporal bone was purchased (Science Care, Phoenix, AZ) and drilled to optimize the resolution of the scan. Figure 2 shows a micro CT scan image (SkyScan 1172; Bruker microCT, Belgium) of a human cadaveric ear. The distance between the RWM and the basilar membrane was estimated to be 1.2 mm. Therefore, the optimal length of the wedge was determined to be 0.6 mm so that the wedge has enough sharpness to penetrate a RWM.

Adjacent to the wedge portion of the needle, there is a 0.4 mm length of “slide and stop” region where the insertion of the needle is stopped (Figure. 1); at this point, the needle is positioned to start sampling. This region is sufficiently larger than the inner diameter such that the hole in the needle is completely in the scala tympani being ready for perilymph

Author Manuscript Author Manuscript Author Manuscript Author Manuscript

aspiration. Also, it is 0.11 mm thinner than the outer diameter of the original 31G needle, meaning the perforation in the RWM will be narrower.

To facilitate rapid aspiration of perilymph solution with negligible pressure, fluid dynamics was considered, and the dimension of the needle was determined as follows. While smaller needle diameter minimizes RWM trauma, the time necessary for the aspiration increases. When a 31-gauge needle is used for aspiration, the pressure necessary for fluid to enter the needle can be estimated by applying Poiseuille's law:

$$\Delta P = \frac{8\mu L Q}{\pi r^4} \quad (1)$$

where, the pressure, ΔP, necessary to carry 1 μL of Newtonian fluid, with viscosity of μ=0.001 Pa*s, through a tube of radius r=100 μm, at the volume rate of Q: 0.01 mm^3/s =1 μL/100s, is 25.4 Pa (=2.5 mmH_2O). This dimension will provide negligible hydrodynamic resistance for the aspiration of perilymph solution.

B. Manufacturing and evaluation

Wire electro discharge machining (EDM) R40 (Mitsubishi, Japan) was used to fabricate the dual wedge needles. A medical grade stainless steel 31 gauge hypodermic needle was purchased from Small Parts (Logansport, IN). The needle was fixed using a specialized jig aligned precisely along the 3 dimensional coordinate system of the EDM. A cutting path consisting of one rough cut followed by 4 skim cuts was determined to define the dual wedge needle from the longitudinal plane view. The 4 skim cuts were required to improve the precision and minimize surface roughness.

The roughness and sharpness of the dual wedge needle was evaluated with 3-D Optical Surface profilers, NewView 7400 (Zygo, CT). The surface topography was obtained first from the frontal and transverse plane views of the dual wedge needle. Using topographical data from the frontal plane view, the root mean square roughness of the cutting surface was calculated using MetroPro (Zygo, CT). The surface roughness of a hypodermic needle was used as a control. The sharpness was quantified as the curvature radius of the wedge tip. In the transverse plane view, in which the needle tip was looked down, the 3D shape of the edge of the two linear blades was obtained such that the topography of the whole length of the wedge tips could be determined. Using MATLAB (Mathwork, MA), the mean cross section of the wedge shape along the whole length was calculated. A quadratic curve fit was performed on the mean cross section, and the inverse of the second derivative of the function was used as a curvature radius.

C. Sampling precision confirmation

The precision of the sampling method was confirmed by measuring the weight of the sampled solution 20 times using an analytical scale, PI-214A (DENVER, NY), at the precision of 0.1 mg. The prototyped dual wedge needle was attached to a 30G polyimide tube (Small parts, IN) followed by a 10 μL micropipette tip (Eppendorf, Germany) using 2 ton epoxy glue (Devcon, MA). Using an Eppendorf micropipette, 1.0μL of saline solution

Author Manuscript Author Manuscript Author Manuscript Author Manuscript

was sampled through the wedge needle and ejected into a microcentrifuge tube (Cole-Parmer, IL). Given that the density of saline solution is 1.0046g/mL, this scale provides 0.1μL precision in volume measurement. The average ejection weight was 0.995 mg with a standard deviation of 7.6%.

D. In vitro demonstration with a guinea pig cochlea

Guinea pigs with no history of middle ear disease were euthanized under pentobarbital anesthesia in accordance with the guidelines of the Institutional Animal Care and Use Committee (IACUC) at Columbia University (N=3). Immediately after euthanization, both temporal bones were isolated and placed in a bottle with enough moisture. These 6 bones were drilled to expose the cochlea and further trimmed to remove the bone hanging over the RWMs. The cochlea bones were fixed on a petri dish using wax and the petri dish was filled with saline solution to provide moisture. The dual wedge needle was lowered slowly under the control of a micromanipulator to puncture the RWM. Penetration of the RWM was confirmed with binocular microscopy. The needle was advanced until the wedge was positioned completely in the perilymphatic space. The micropipette attached to the dual wedge needle was used to aspirate 1 μL of perilymph solution. After the aspiration, the dual wedge needle was retracted. The aspirated perilymph solution was ejected into 39 μL of saline solution in a microcentrifuge tube.

In this *in vitro* experiment, these bulla bones were isolated from the skull such that there was no CSF pressure through the cochlear aqueduct. During the penetration and aspiration, the wax blocked the aqueduct preventing the air entry into the inner ear. This preparation ensured that sampling of the inner ear solution via the RWM would provide only perilymph solution without CSF contamination.

Immediately after the sampling experiment, the inner ears were fixed in a 10% neutral buffered formaldehyde solution overnight and underwent dehydration for scanning electron microscopy as previously described (19). Briefly, after dehydration using ethanol, critical point drying was performed with hexamethyldisiloxane. After applying a thin coating of gold, scanning electron microscopy was performed to determine the shape and size of the incision.

E. UV-Vis absorbance spectroscopy of sampled guinea pig perilymph solution for protein analysis

To confirm the success of sampling the perilymph and to demonstrate the feasibility of protein analysis, the sample perilymph was analyzed via UV-Vis absorbance spectroscopy using a plate reader Synergy 4 (Biotek®, VT). The solution was kept temporarily in a microcentrifuge tube and mixed with a vortex mixer. The 20 μL solution was transferred to a Corning® 96 well UV plate with flat bottoms (Sigma-Aldrich) and an additional 20 μL saline solution was poured in. The plate reader procedure was 30 seconds of shaking followed by absorption spectroscopy of UV and visible light (200 ~800 nm). The concentration of protein mixtures was roughly estimated by the following formula

Author Manuscript Author Manuscript Author Manuscript Author Manuscript

$$X = \mathrm{A}/\mathrm{L} \quad (2)$$

where X: the concentration (mg/mL), A: absorbance (dimension less number), and L: path length (cm) (20,21). The path length of the specimen was calculated as 0.63 mm by dividing the volume (40 μL) by the surface area of the bottom using the diameter of 6.35 mm. The ratio of the dilution was taken into account.

III. Results

A. Prototype dual wedge needle

Via the wire EDM, the designed shape was successfully fabricated (Figure 3). Figure 3 (a) shows the assembled needle system for sampling perilymph solution using a micropipette. The polyimide tube in the middle was used for flexibility and to form a tight fit with the dual wedge needle, thus ensuring a leakless connection. In this study, an oversize stainless steel tube was put on over the polyimide tube to stabilize the needle during the penetration of the guinea pig RWM.

Figure 4 shows the topography of one of the dual blades of the needle captured from the frontal view plane. The surface roughness was 3.66 μm in root mean square. By contrast, the surface roughness of a hypodermic needle was 3.15 μm (topographical data not shown). The cutting surface made by the wire EDM was as smooth as a standard hypodermic needle. In Figure 5, the green line shows the average profile of the cross section of the tip of the wedge needle in the longitudinal plane view. The blue dashed line is the quadratic fit curve. The curvature radius of the tip was as small as 4.5 μm.

B. Linear incision in the guinea pig RWM

Figure 6 shows optical micrographs captured through the eyepiece of a binocular microscope before and after penetration of a RWM. Being pushed by the wedge needle, the RWM deformed and stored elastic energy until the needle penetrates the RWM. The moment of initial penetration was easily confirmed visually when the RWM slightly rebounded. Further penetration was immediately terminated, ensuring that penetration of the RWM did not exceed the point of the needle stopper. Because the penetration was performed always in the center of the RWM at right angle and the precision in the needle, the needle had enough clearance from damaging the other inner ear structure. The aspiration took less than a few seconds (need to define time), and (is there a word missing here?) small deformation of the RWM or change in the level of water were observed during the aspiration process.

Electron microscopy following perforation showed an intact RWM with an oval shaped hole (Figure 7a). The average major and minor axis diameters of the perforation were 344 and 143 μm, with a standard deviation of 37.9 and 26.5 μm (11% and 19%). Pearson's r between the major and minor diameter was 0.4. These two types of values suggest that the size of hole varies with small geometrical similarity. The aspect ratio was 0.416 with standard deviation of 6.7%. When we compare the groups of major diameters multiplied by 0.4 with the minor diameters, the t-value for a 95% confidence was 0.013. This value confirms the

Author Manuscript Author Manuscript Author Manuscript Author Manuscript

consistency of the oval shape of the perforation made by the prototype needle. Figure 7 (b) shows a comparable optical micrograph of a RWM with a hole penetrated manually by an insect pin with a diameter of 100 μm. Typically, the hole expands as great as 5 times in both the major and minor axes when a round needle penetrates the RWM of a guinea pig.

C. The concentration of protein in the perilymph incision

Figure 8 shows the absorbance spectroscopy of the sampled perilymph solution, saline solution, and the subtraction curve of the two curves in blue, red, and green in the wavelength range of 240 to 320 nm. From the t-value of the two curves, a significant difference was clear, suggesting the presence of the protein. The subtraction curve showed peaks of 0.39 and 0.030 at 205 and 270 nm. The absorbance at 280 nm was 0.027. From this absorbance value at 280 nm, the protein concentration was estimated to be 1.74 mg/mL.

IV. Discussion

We are on the cusp of developing disease specific therapies for inner ear disorders (13-16). To implement personalized medicine, we could take advantage of specific affinity properties of carrier materials to target tissues, cell-specific receptors and promoters, or the restricted biochemical reactiveness of proteins in cells. However, for any given patient, we are hindered by the absence of a precise diagnosis for their underlying auditory and/or vestibular disturbance. This, in part, could be overcome by having inner ear fluid available for diagnostic testing. Inner ear diagnostics performed on cochlear fluids could elucidate the etiology more precisely, thus allowing directed therapeutics to be administered. In this study, we designed, built, and tested a dual wedge needle for perforating the RWM and aspirating perilymph. The needle created precise replicable RWM holes, and facilitated rapid and controlled aspiration of perilymph.

A. Design and production of the needle

The production method using wire EDM was adequate and appropriate for the design. Of note, the more conservative manufacturing process of grinding used to manufacture hypodermic needles can also be used to reproduce the dual wedge needle, thus minimizing cost, allowing scalability, and being compatible with clinical use.

With the dual wedge needle, the penetration of a guinea pig RWM was smooth and the size of perforation consistent across trials. The wedge shaped needle facilitated precise and quick sampling of perilymph without inner ear trauma. A flexible polyimide tube was used with the needle as any aspiration tool will need to accommodate the curved nature of the human external auditory canal and the orientation of the RWM (Figure 1). Thus, the final design will need to include a curved shape to orient the tip for the penetration of the RWM at a right angle. A Rosen needle is an example of current surgical tools that has a curved tip. Within the body of the curved surgical tool, this flexible polyimide tube can be embedded to account for the three dimensional anatomy of the ear.

Author Manuscript Author Manuscript Author Manuscript Author Manuscript

B. Atraumatic sampling: Force required to penetrate, Shape of the hole

Previous studies using guinea a pig model show that larger holes in RWMs than the holes seen in this study heal spontaneously within a few days without significant damage to hearing (25-29). Our results demonstrated that the designed needle is capable of leaving incisions of an oval shape with the minor axis diameter smaller than the diameter of a 31 gauge needle. A healthy RWM is under pre-tension and, without proper care, penetration can rip a hole, causing catastrophic rupture and resulting in complete loss of the RWM. The consistent size and shape of the perforation in this study demonstrated that the sampling method using the prototype needle minimized such a risk. Further *in vivo* experiments using guinea pig models will follow to assess the level of damage in terms of the duration necessary for healing as well as any loss of hearing. The human RWM has a much larger size than that of a guinea pig. Our preliminary experience of penetrating a human RWM using the prototype needle showed better chances of minimizing the trauma due to the human RWMs being structurally stronger than guinea pig's RWMs. Another consideration is it is ideal to have a safety mechanism to prevent the contact of the needle tip to the inner ear structure such as the basilar membrane. This function can be complemented by a feedback system utilizing a proximity sensor (30).

C. Precise and quick sampling

The 31 gauge needle used in this study has small enough fluidic resistivity to aspirate the 1 μm of perilymph solution within a few seconds with great accuracy. This fluidic resistivity provides enough room to further improve the atraumacity of perilymph sampling since it is easier to reduce the speed of aspiration than to increase it. In addition to precise control over the volume of the perilymph sample, minimizing intrascalar pressure is also critical for atraumacity of the inner ear structure. Complications can be caused by intracochlear pressure changes in cases of cochlear implantation, Meniere's disease, or barotrauma experienced by divers. While minimizing the volume of perilymph solution removed alone will reduce the risk of physical damage caused by pressure, slowing down the aspiration will likely minimize the pressure and the risk as well.

The volume of the human scala tympani is on the order of a 44 μL (22). Thus, 1.0 μL of perilymph removal is 2.2% of the entire volume. Although *in vivo* study with experimental animals is required to determine the level of damage caused by the volume of perilymph withdrawn, 1.0 μL of perilymph removal seems to be a reasonable starting volume. The scala tympani is connected to the scala vestibuli through helicotrema and the partially sealed cochlea aqueduct next to the RWM that communicates moderately with cerebrospinal fluid. The fluidic conductance through these routes is limited and the dynamic pressure grow proportionally to the fluidic resistance as well as the speed of fluidic flow. Although, the perilymph flow rate in a healthy human individual is not yet known, the flow rate of a guinea pig is known to be 0.001 to 1 μL/min (23,24). Therefore, we are currently developing a pressure, flow rate, and volume control system to slow the aspiration speed from 0.3 μL/sec down to 0.01 μL/sec. Further, this aspiration method will be evaluated with an intrascalar pressure sensing experiment.

Author Manuscript Author Manuscript Author Manuscript Author Manuscript

D. Molecular analysis of the sampled perilymph solution

We showed that the sampled fluid was a biological solution by confirming the presence of proteins via absorbance spectroscopy. The value of 1.74 mg/mL falls within the range of literature values:1.50 (31) and 2.757 ± 0.238 mg/mL (5). Although, the biochemical analysis is not the goal of this study, the protein constituents of sampled solution can be analyzed and identified via LC-MS/MS (32,33). In a guinea pig model, 1 μL of perilymph solution sampled via the RWM contains 10 % of CSF (34). Although the cochlear aqueduct of a human is normally blocked and the contamination of CSF is small, it may be interesting to determine the proportion of the CSF to perilymph in the sampled solution from the guinea pig *in vivo* using LC-MS/MS.

V. Conclusion

We have designed a microneedle with a dual wedge at the tip using a 31G needle for the sampling of perilymph solution through the RWM with minimal damage. Using a wire EDM, the designed needle was fabricated with high quality, i.e. meaning excellent sharpness at the tip and a smooth surface. A precise aspiration system was developed utilizing a micropipette. Using this aspiration system, we demonstrated sampling of perilymph from a guinea pig cochlea while leaving a controlled oval perforation.

Acknowledgments

This research was funded by Coulter Translational Research Partnerships and American Otological Society. Professor Elizabeth S. Olson Ph.D. has been kindly providing her lab space as well as her knowledge. This research was supported by NIH National Institute on Deafness and Other Communication Disorders of the National Institutes of Health under award number R01DC014547.

References

1. Silverstein H. A rapid protein test for acoustic neurinoma. Arch Otolaryngol. 1972; 95:202–4. [PubMed: 5013262]
2. Silverstein H. Labyrinthine tap as a diagnostic test for acoustic neurinoma. Otolaryngologic clinics of North America. 1973; 6:229–44. [PubMed: 4220279]
3. Arrer E, Oberascher G, Gibitz HJ. A map of cochlear perilymph protein based on high-resolution two-dimensional electrophoresis. Eur Arch Otorhinolaryngol. 1990; 247:271–3. [PubMed: 2393558]
4. Paugh DR, Telian SA, Disher MJ. Identification of perilymph proteins by two-dimensional gel electrophoresis. Otolaryngology-- head and neck surgery : official journal of American Academy of Otolaryngology-Head and Neck Surgery. 1991; 104:517–25. [PubMed: 1710047]
5. Thalmann I, Comegys TH, Liu SZ, et al. Protein profiles of perilymph and endolymph of the guinea pig. Hearing research. 1992; 63:37–42. [PubMed: 1464573]
6. Thalmann I, Kohut RI, Ryu J, et al. Protein profile of human perilymph: in search of markers for the diagnosis of perilymph fistula and other inner ear disease. Otolaryngology--head and neck surgery : official journal of American Academy of Otolaryngology- Head and Neck Surgery. 1994; 111:273–80. [PubMed: 8084635]
7. Chiarella G, Di Domenico M, Petrolo C, et al. A proteomics-driven assay defines specific plasma protein signatures in different stages of Meniere's disease. Journal of cellular biochemistry. 2014; 115:1097–100. [PubMed: 24356812]
8. Chiarella G, Saccomanno M, Scumaci D, et al. Proteomics in Meniere disease. Journal of cellular physiology. 2012; 227:308–12. [PubMed: 21437900]

Author Manuscript Author Manuscript Author Manuscript Author Manuscript

9. Kitahara T, Doi K, Maekawa C, et al. Meniere's attacks occur in the inner ear with excessive vasopressin type-2 receptors. Journal of neuroendocrinology. 2008; 20:1295–300. [PubMed: 19094077]
10. Maekawa C, Kitahara T, Kizawa K, et al. Expression and translocation of aquaporin-2 in the endolymphatic sac in patients with Meniere's disease. Journal of neuroendocrinology. 2010; 22:1157–64. [PubMed: 20722976]
11. Lysaght AC, Kao SY, Paulo JA, et al. Proteome of human perilymph. Journal of proteome research. 2011; 10:3845–51. [PubMed: 21740021]
12. Britze A, Birkler RI, Gregersen N, et al. Large-scale proteomics differentiates cholesteatoma from surrounding tissues and identifies novel proteins related to the pathogenesis. PloS one. 2014; 9:e104103. [PubMed: 25093596]
13. Surovtseva EV, Johnston AH, Zhang W, et al. Prestin binding peptides as ligands for targeted polymersome mediated drug delivery to outer hair cells in the inner ear. International Journal of Pharmaceutics. 2012; 424:121–7. [PubMed: 22227343]
14. Mizutari K, Fujioka M, Hosoya M, et al. Notch Inhibition Induces Cochlear Hair Cell Regeneration and Recovery of Hearing after Acoustic Trauma. Neuron. 2013; 78:403.
15. Jero J, Mhatre AN, Tseng CJ, et al. Cochlear gene delivery through an intact round window membrane in mouse. Human Gene Therapy. 2001; 12:539–48. [PubMed: 11268286]
16. Buckiová D, Ranjan S, Newman TA, et al. Minimally invasive drug delivery to the cochlea through application of nanoparticles to the round window membrane. Nanomedicine. 2012; 7:1339–54. [PubMed: 22475648]
17. Thomas PV, Cheng AL, Colby CC, et al. Localization and proteomic characterization of cholesterol-rich membrane microdomains in the inner ear. Journal of proteomics. 2014; 103:178–93. [PubMed: 24713161]
18. Darville LN, Sokolowski BH. Bottom-up and shotgun proteomics to identify a comprehensive cochlear proteome. Journal of visualized experiments : JoVE. 2014
19. Watanabe H, Kysar JW, Lalwani AK. Microanatomic analysis of the round window membrane by white light interferometry and microcomputed tomography for mechanical amplification. Otology & neurotology : official publication of the American Otological Society, American Neurotology Society [and] European Academy of Otology and Neurotology. 2014; 35:672–8.
20. Layne, E. Methods in Enzymology. Academic Press; 1957. [73] Spectrophotometric and turbidimetric methods for measuring proteins; p. 447-54.
21. Stoscheck, CM. [6] Quantitation of protein. In: Murray, PD., editor. Methods in Enzymology. Academic Press; 1990. p. 50-68.
22. Igarashi M, Ohashi K, Ishii M. Morphometric comparison of endolymphatic and perilymphatic spaces in human temporal bones. Acta oto-laryngologica. 1986; 101:161–4. [PubMed: 3518332]
23. Ohyama K, Salt AN, Thalmann R. Volume flow rate of perilymph in the guinea-pig cochlea. Hear Res. 1988; 35:119–29. [PubMed: 3198505]
24. Salt AN, Inamura N, Thalmann R, et al. Evaluation of procedures to reduce fluid flow in the fistulized guinea-pig cochlea. Acta otolaryngologica. 1991; 111:899–907.
25. Axelsson A, Hallen O, Miller JM, et al. Experimentally induced round window membrane lesions. Acta oto-laryngologica. 1977; 84:1–11. [PubMed: 899747]
26. Gyo K. Healing of experimentally produced round window membrane rupture. Acta oto-laryngologica. 1989; 107:85–9. [PubMed: 2929319]
27. Lamm K. [Experimental defects of the round window membrane]. Hno. 1992; 40:374–80. [PubMed: 1429026]
28. Lamm K, Lamm H, Lamm C, et al. [Microperforation and removal of the round window membrane. Short- and long-term study in animal experiments using electrocochleography and evoked response audiometry]. Hno. 1988; 36:106–10. [PubMed: 3360631]
29. Sone M. Pathological features of healing of a ruptured human round window membrane. ORL; journal for oto-rhino-laryngology and its related specialties. 1998; 60:55–7. [PubMed: 9519384]
30. Watanabe H, Velmurugan J, Mirkin MV, et al. Scanning electrochemical microscopy as a novel proximity sensor for atraumatic cochlear implant insertion. IEEE transactions on biomedical engineering. 2014; 61:1822–32. [PubMed: 24845292]

Author Manuscript Author Manuscript Author Manuscript Author Manuscript

31. Scheibe F, Haupt H, Hache U, et al. [Protein concentration in the guinea-pig perilymph]. Acta oto-laryngologica. 1975; 79:51–7. [PubMed: 1146538]

32. Swan EE, Peppi M, Chen Z, et al. Proteomics analysis of perilymph and cerebrospinal fluid in mouse. The Laryngoscope. 2009; 119:953–8. [PubMed: 19358201]

33. Lysaght AC, Kao S-Y, Paulo JA, et al. Proteome of Human Perilymph. Journal of proteome research. 2011; 10:3845–51. [PubMed: 21740021]

34. Salt AN, Hale SA, Plonkte SK. Perilymph sampling from the cochlear apex: a reliable method to obtain higher purity perilymph samples from scala tympani. Journal of neuroscience methods. 2006; 153:121–9. [PubMed: 16310856]

Author Manuscript Author Manuscript Author Manuscript Author Manuscript

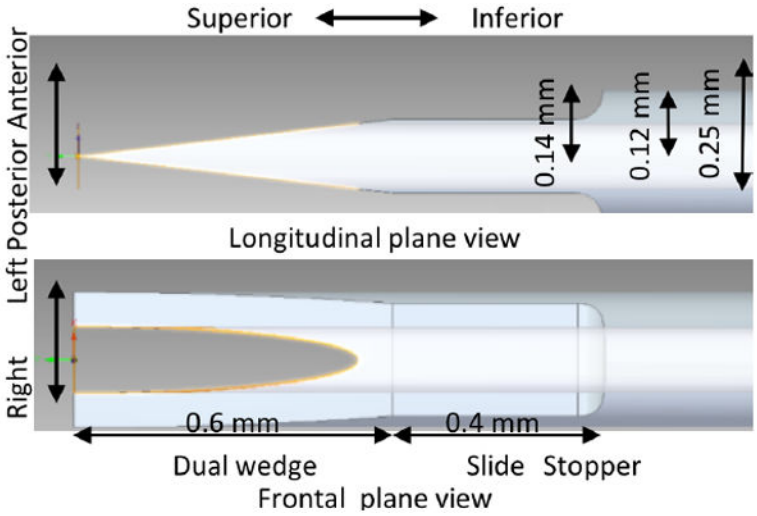

Fig. 1.

The design of the dual wedge needle. The standard terms of location used for animal anatomy was used to describe the directions and planes of the designed needle.

Author Manuscript Author Manuscript Author Manuscript Author Manuscript

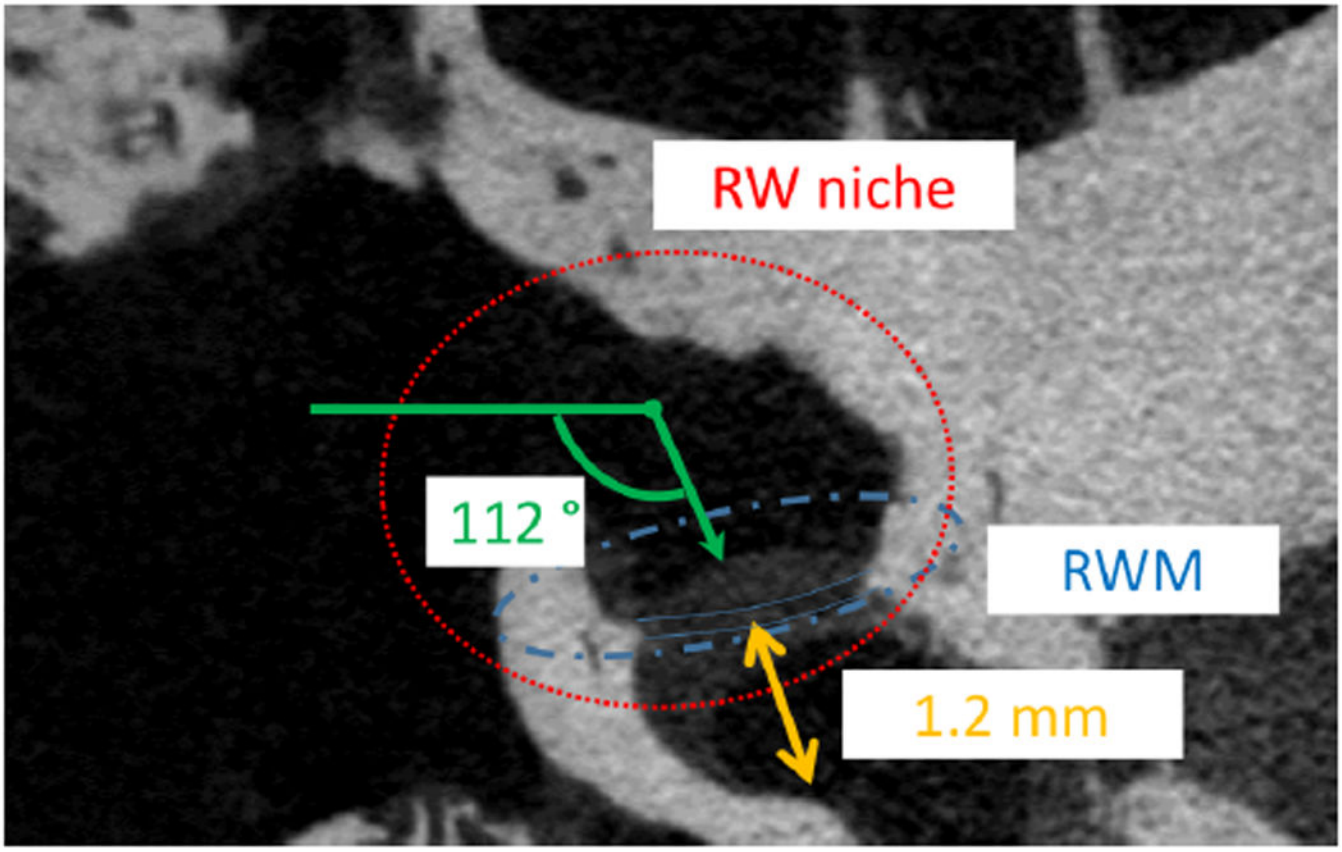

Fig. 2.
A micro CT scan image showing a round window niche and a RWM of a human cadaveric temporal bone.

Author Manuscript Author Manuscript Author Manuscript Author Manuscript

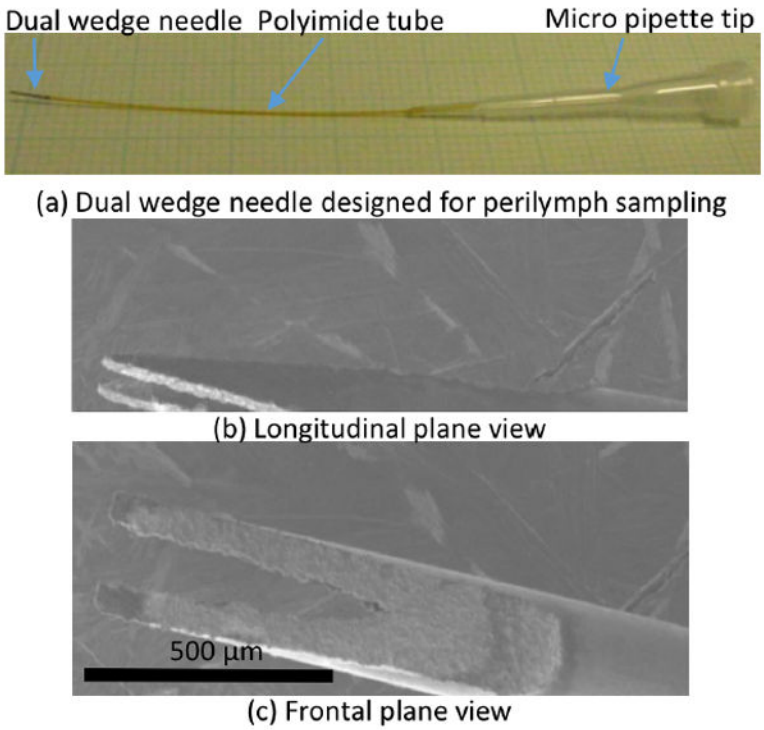

Fig. 3.

(a) An assembled dual wedge needle. From left to right, a dual wedge needle, a flexible Polyimide tube, and a micro pipette tip. (b, c) A scanning electron micrograph of a dual wedged needle manufactured via the wire EDM.

Author Manuscript Author Manuscript Author Manuscript Author Manuscript

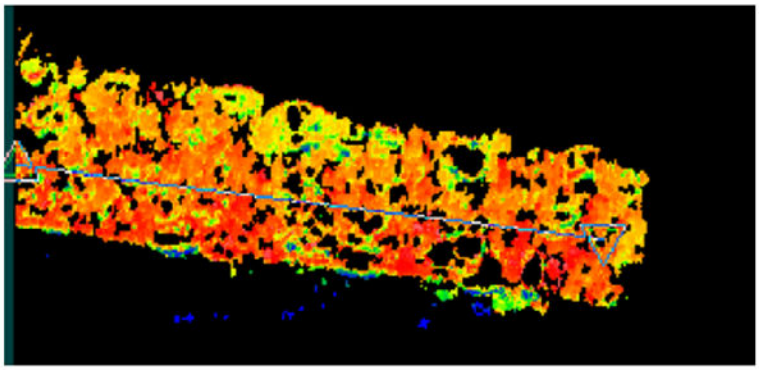

Fig. 4.

The topography of the surface of one blade of the prototyped dual wedge needle. The topography was determined to evaluate the cutting via the wire EDM by surface roughness measurement via Zygo. The blue line segment with triangle marks on both ends indicates the line used for measurement of the surface roughness.

Author Manuscript Author Manuscript Author Manuscript Author Manuscript

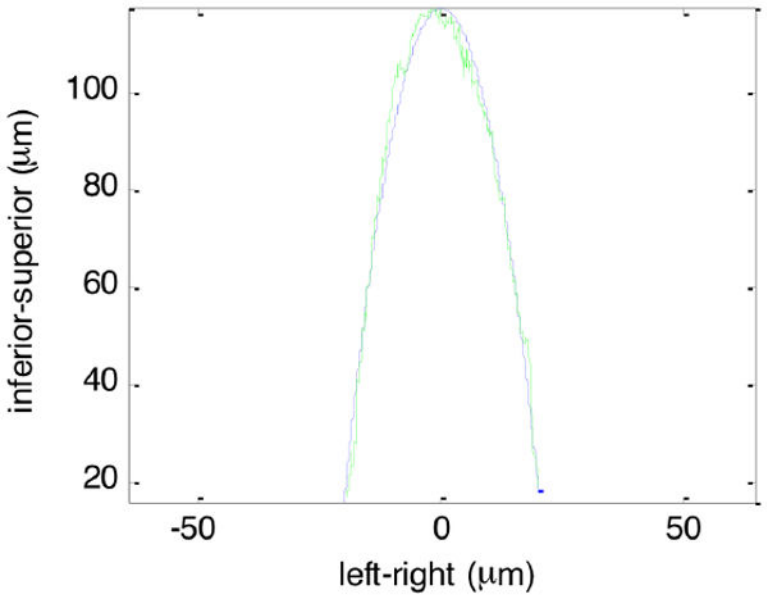

Fig. 5.

The average cross section of the dual wedge needle in green line. The quadratic fit curve in blue broken line.

Author Manuscript Author Manuscript Author Manuscript Author Manuscript

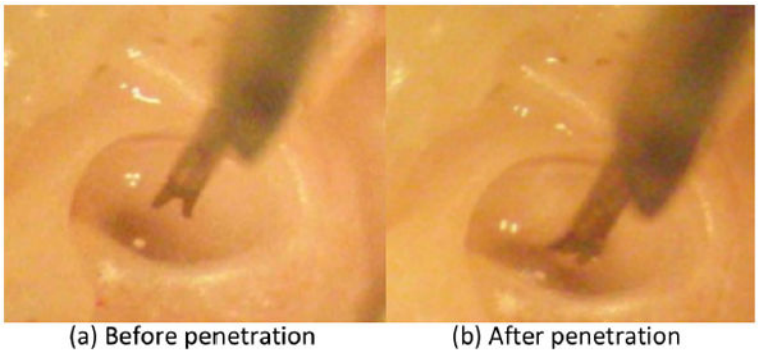

Fig. 6.

Optical micrographs before (a) and after (b) the penetration of a RWM of a guinea pig. (b) the needle tip is in the scala tympani space. Lowering the needle through the RWM was terminated at the stopper.

Author Manuscript Author Manuscript Author Manuscript Author Manuscript

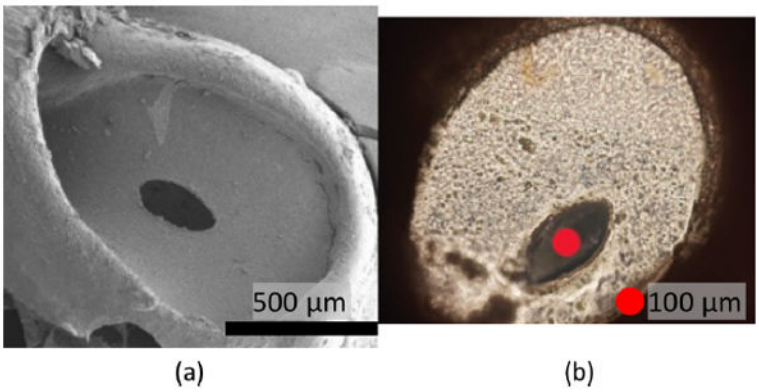

Fig. 7.

(a) Scanning electron micrograph of a guinea pig RWM after sampling of perilymph solution. (b) Optical micrograph of a RWM with a hole made using an insect pin with the diameter of 100 µm.

Author Manuscript Author Manuscript Author Manuscript Author Manuscript

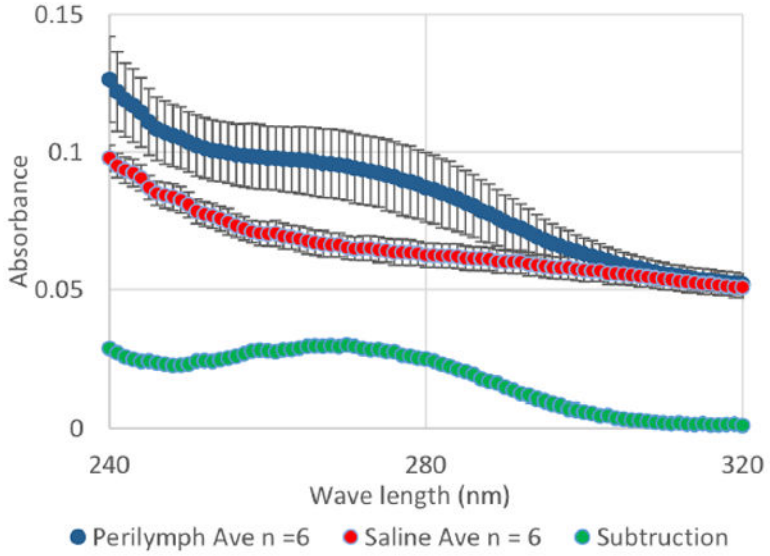

Fig. 8.
UV-Vis spectroscopy of the sampled perilymph (blue) and saline solution (red).